Surface Brightness of Spiral Galaxies

M104: SA

N4535:
SAB

LMC: dwarf irregular,barred

“Normal” 1/4-law+exp fits

An example of surface brightness profile.
The top curve is the sum of exp disk+1/4-bulge.
The bottom curve is 1/4-law for this model.
The dashed line is an exp-law.
Re and Rd are indicated in the plot.

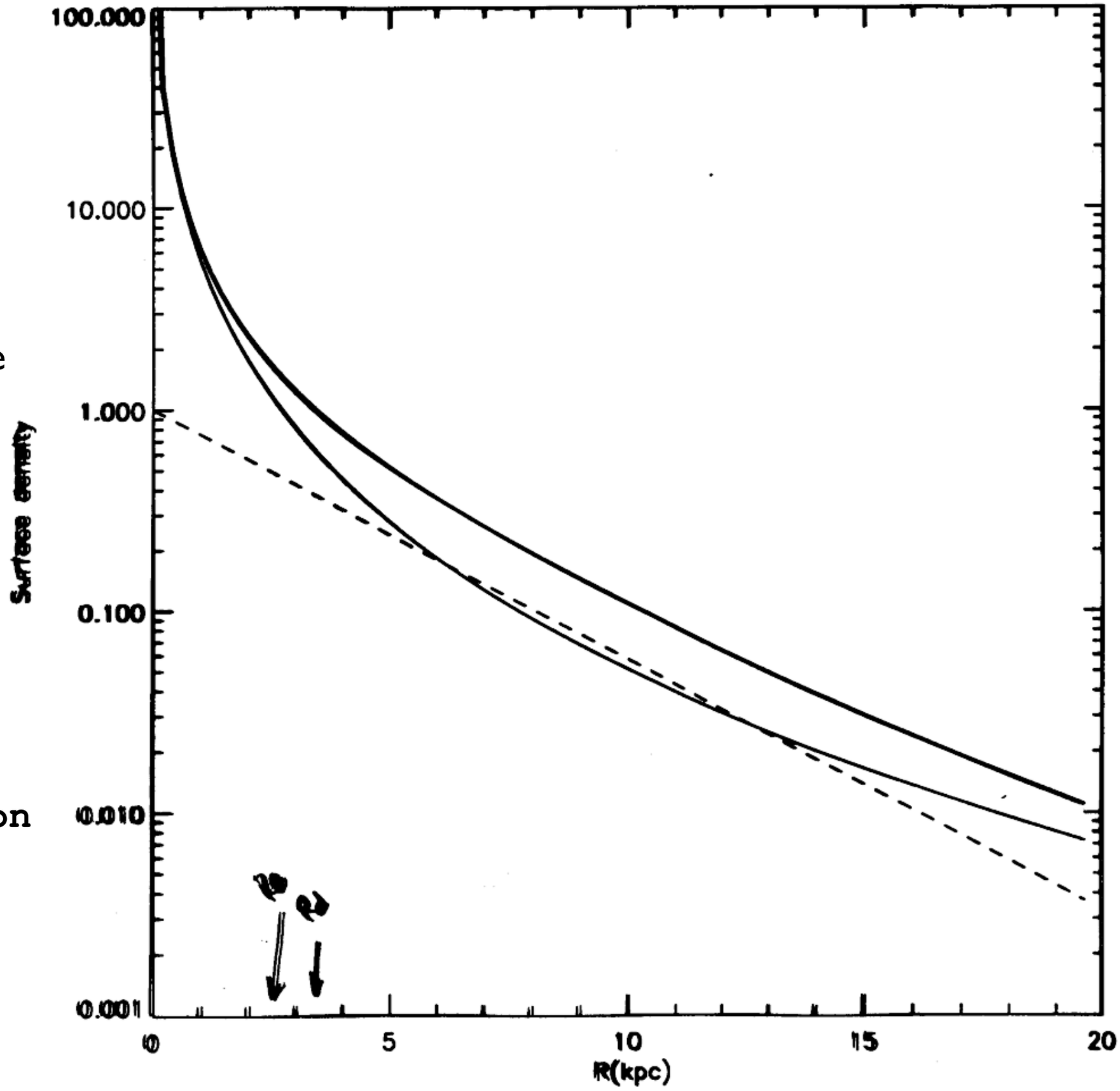

Shapes of bulge and disk profiles are not independent, which makes the decomposition difficult and often unstable

Sersic profiles with different n

Sérsic (1968) generalization:

$$\mu_{ser} = \mu_0 \exp\left[-\left(\frac{r}{r_0}\right)^{\frac{1}{n}}\right]$$

n = 1 ⇒ exponential

n = 4 ⇒ de Vaucouleurs law

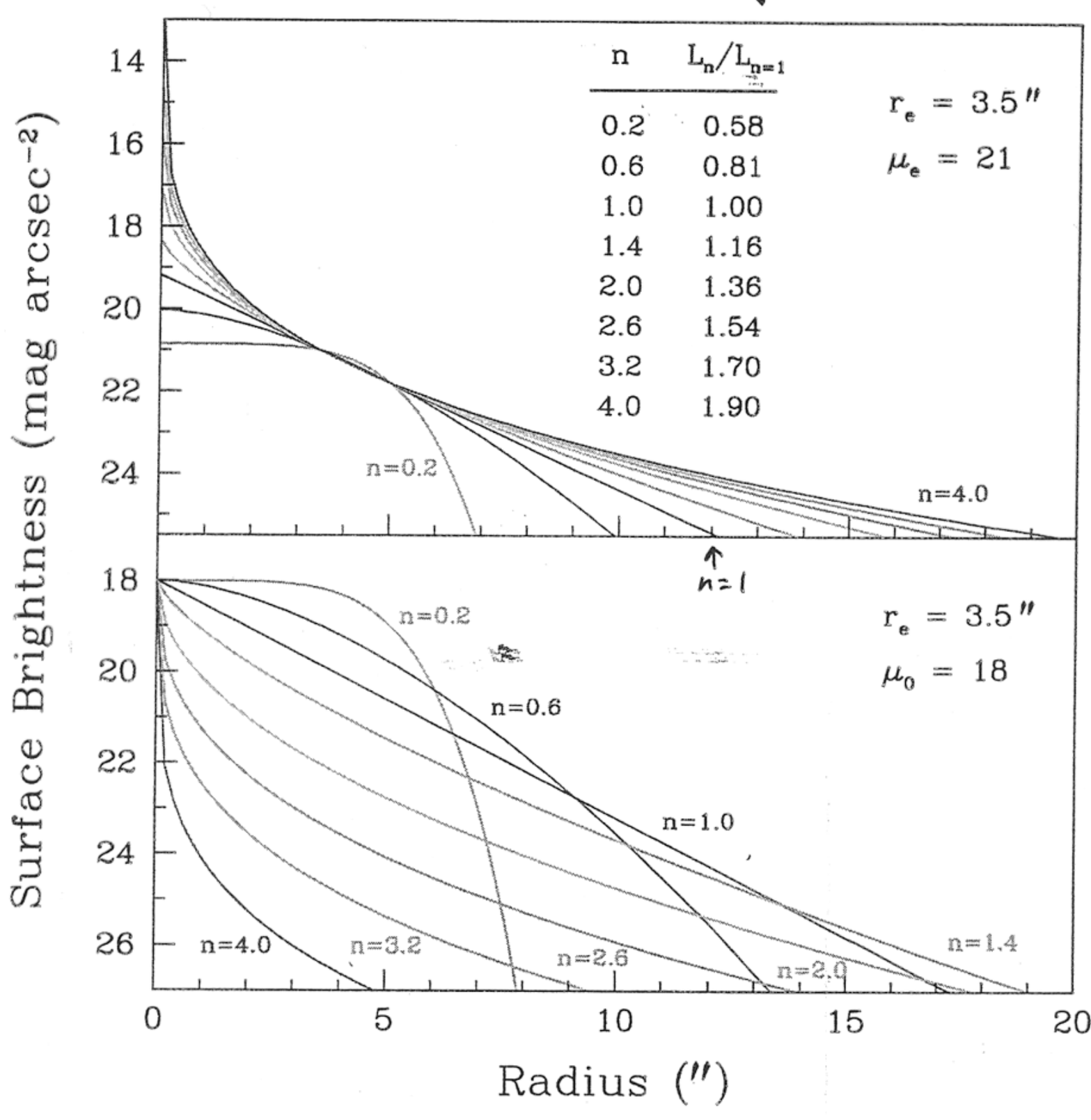

Fig. 2.— Sérsic n profiles for different values of n. The top panel shows profiles with $\mu_e =$ mag arcsec^{-2} and $r_e = 3''.5$ for values of n in the range $0.2 < n < 4$. The table lists t relative light contributions of the different profiles normalized to the $n = 1$ case. The bott panel shows the same profiles except for a constant CSB of $\mu_0 = 18$ mag arcsec^{-2} .

Two types of profiles: FreemanI and FreemanII

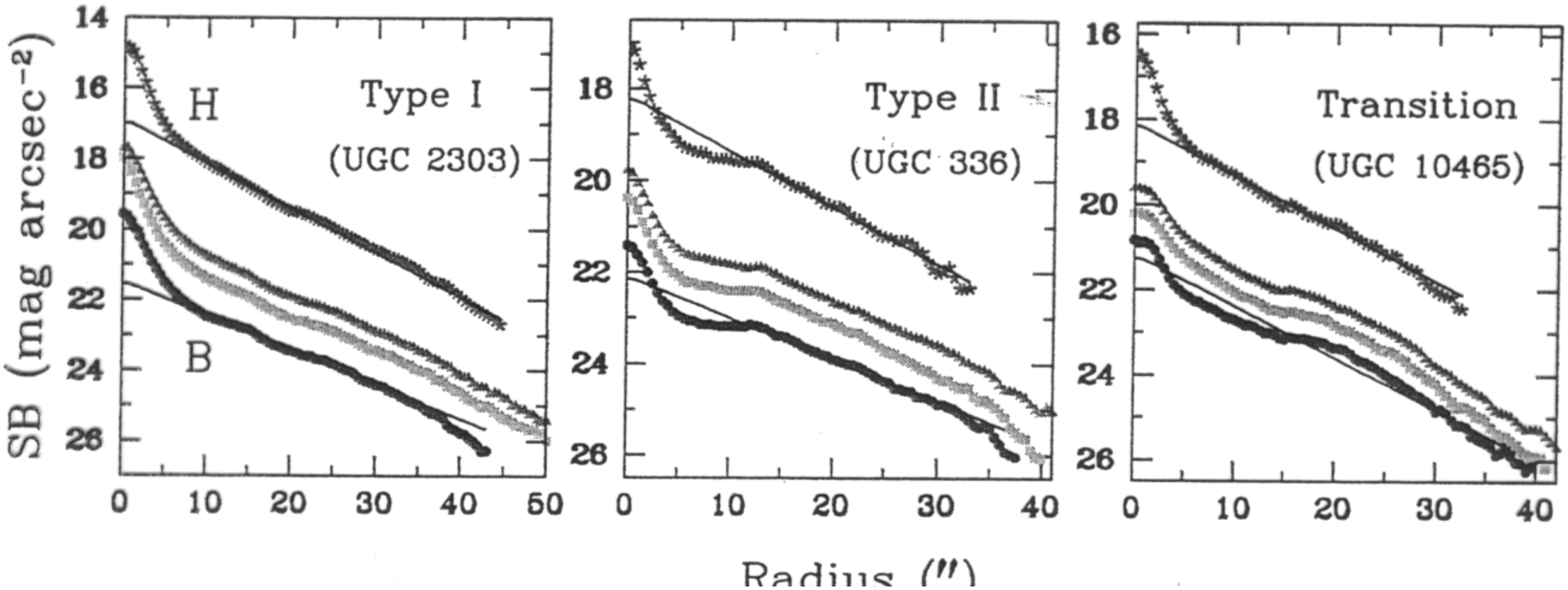

Fig. 1.— Examples of Type-I (left), Type-II (middle), and "Transition" (right) SB profiles. Blue circles, green squares, red triangles, and purple asterisks are for B, V, R, and H-band respectively. The solid black lines plotted on the B-band and H-band profiles are fits to the outer exponential disk profile.

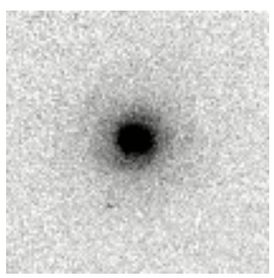

Type:SABb

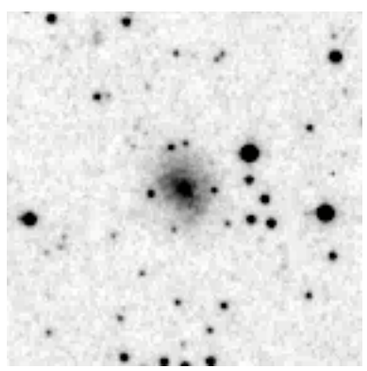

Type:SA

M31 decomposition

Walterbos, Kennicutt 88, A&A 198, 61 exp + "r^1/4"

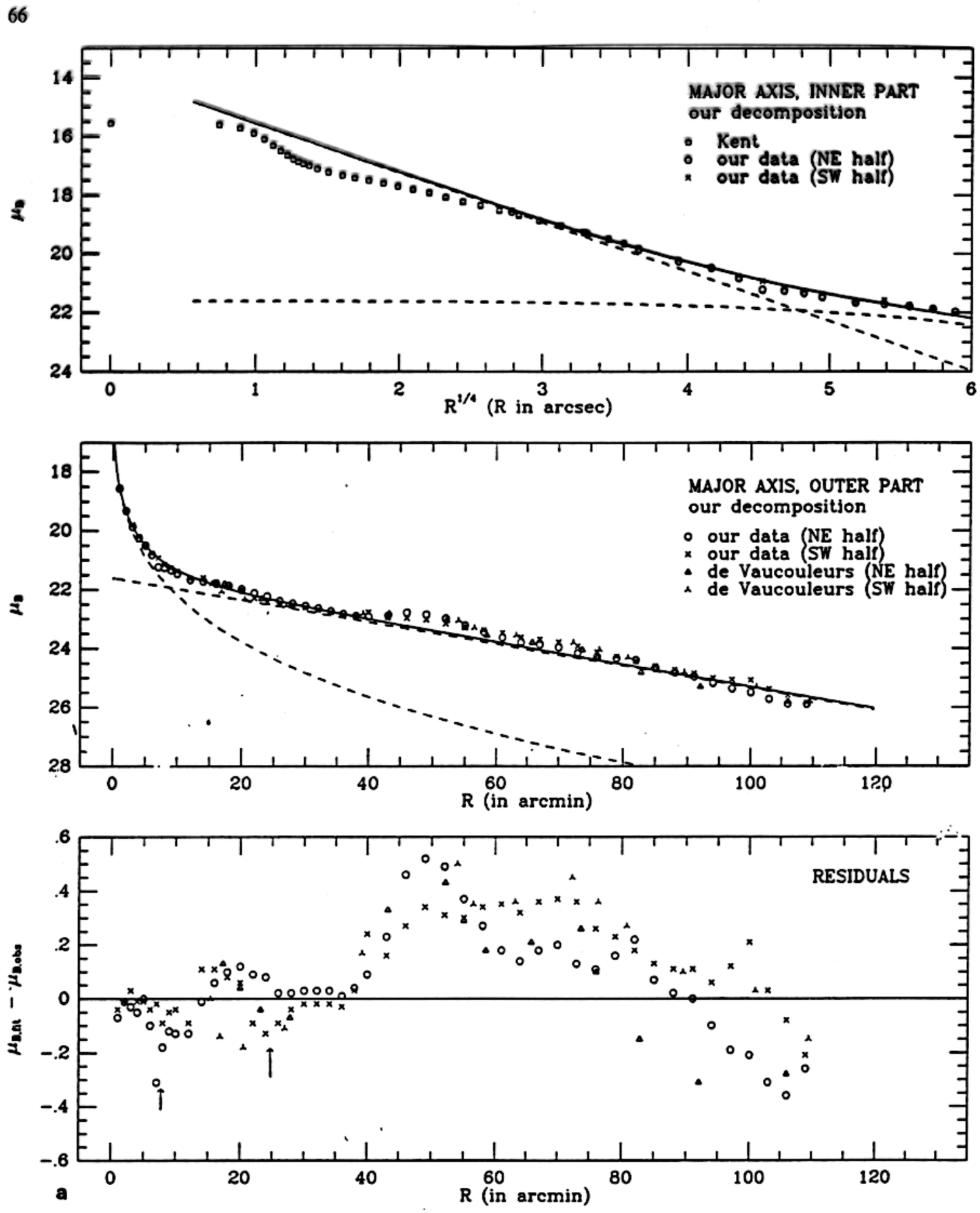

Profiles: examples and fits

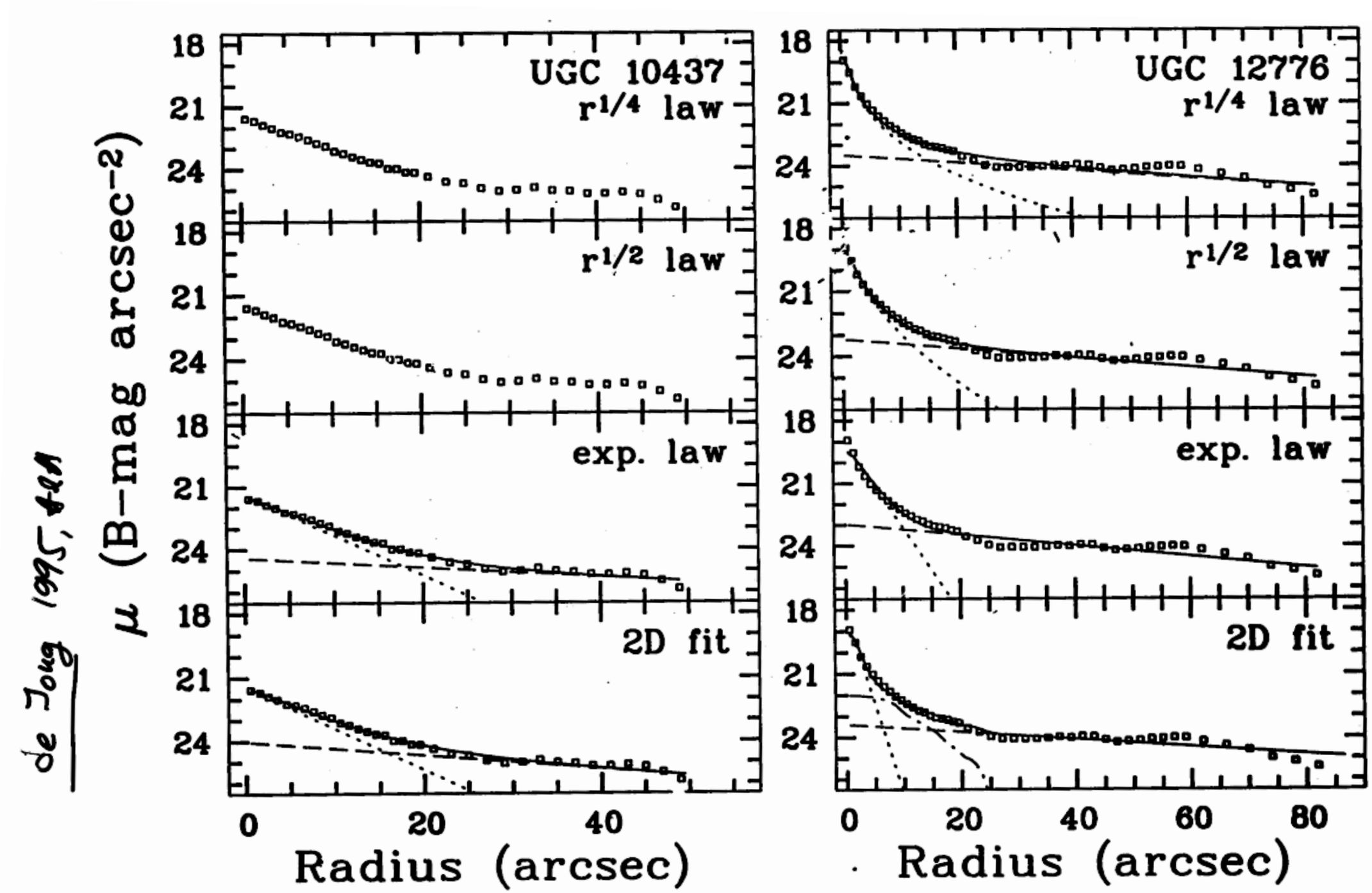

1/4-law is a bad fit

1/4-law is OK

More examples: decompositions are often degenerate

1995

R.S. de Jong: Near-IR and optical observations of 86 spirals. II Determination of bulge and disk parameters

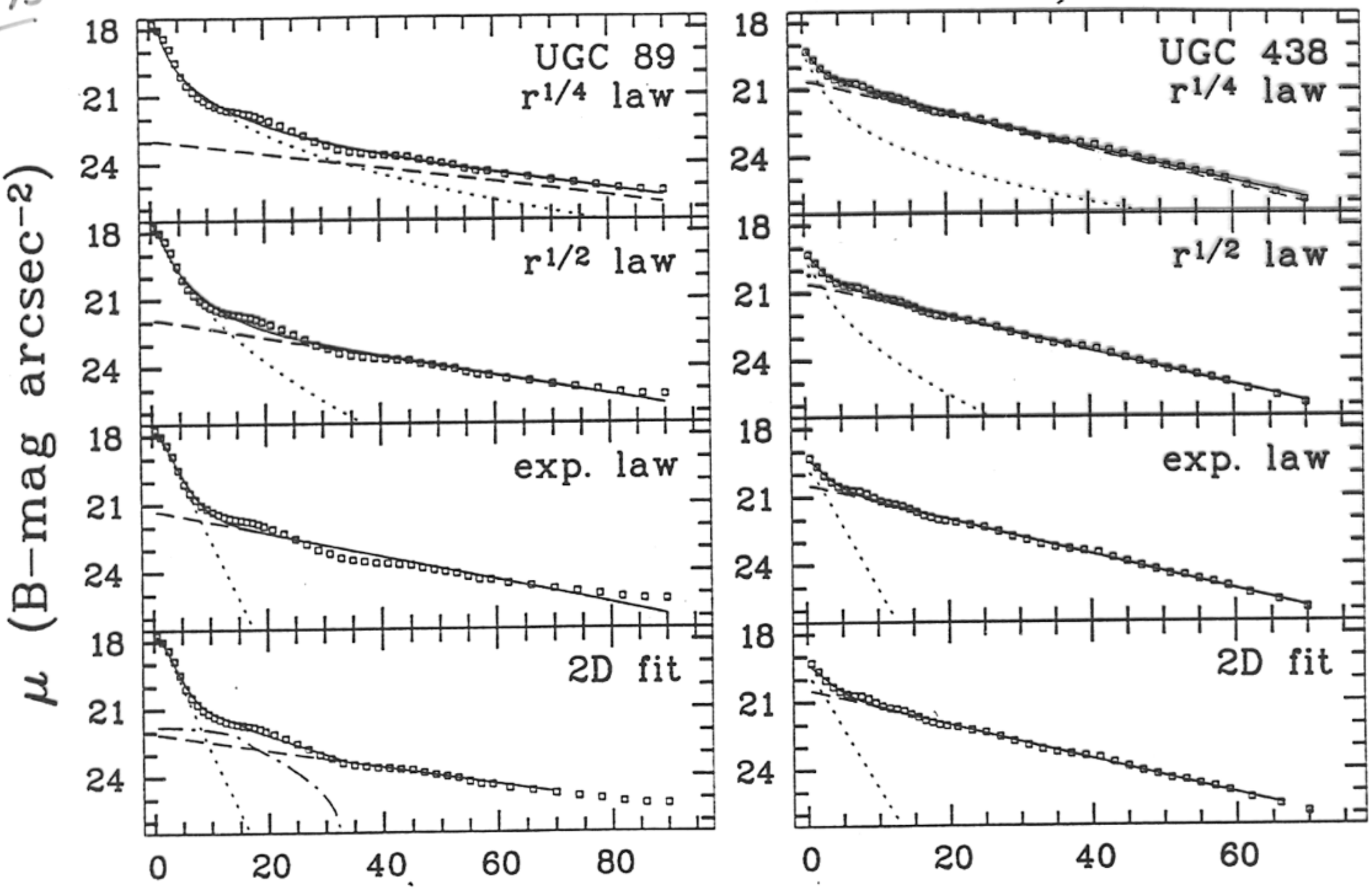

Bulge-to-disk decomposition of a bulge-less galaxy in different color bands. Note that the disk scale length is shorter in red color as compared with blue bands.

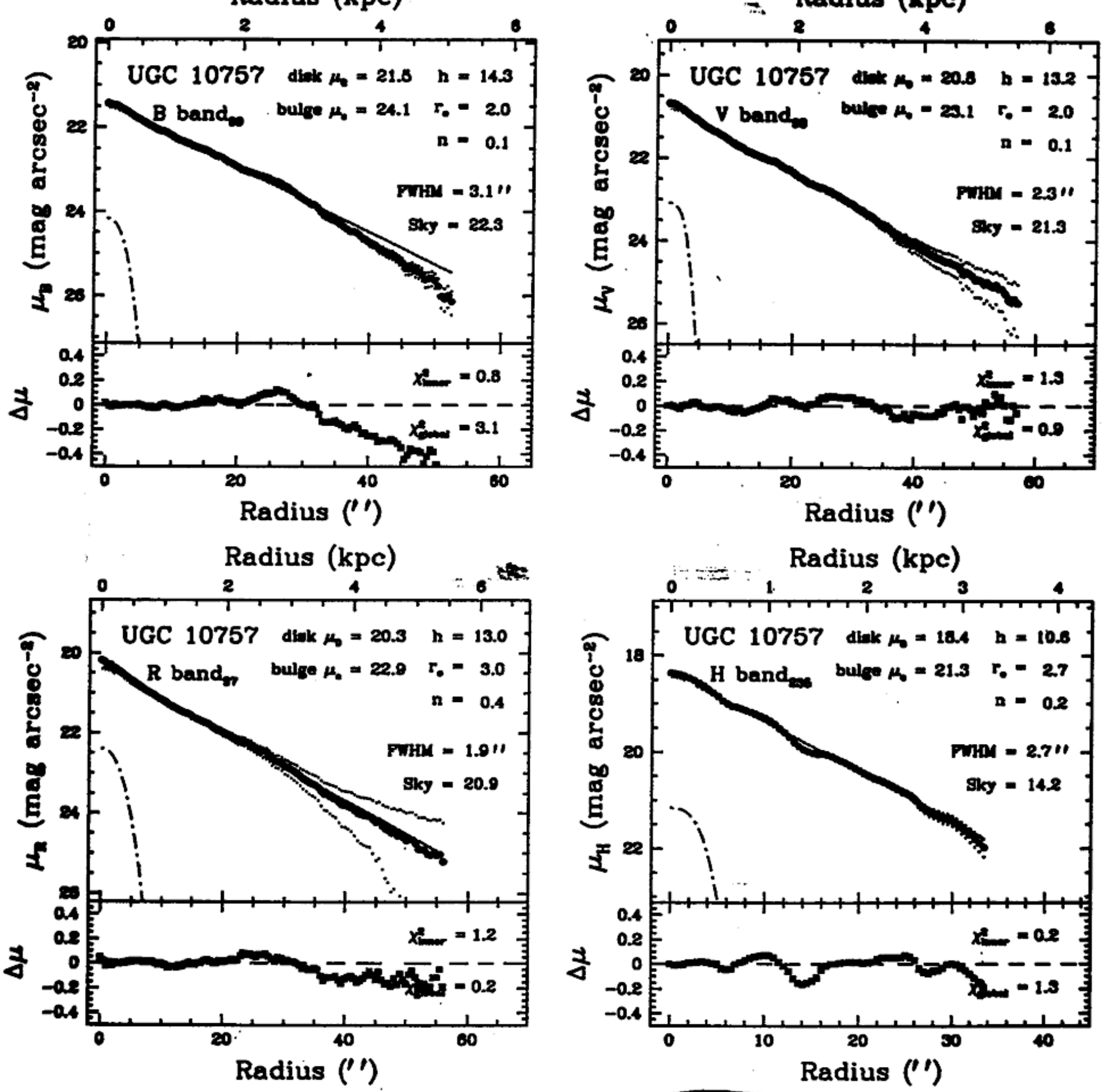

Fig. 14.— Decomposition results for a galaxy with a "bulgeless" disk (UGC 10757).

Bulge-to-disk decomposition.
Bulge is very small.
This is an example of outer disk truncation.
M33 is another example of this type of disk.

Again, the disk scale length gets shorter in red.

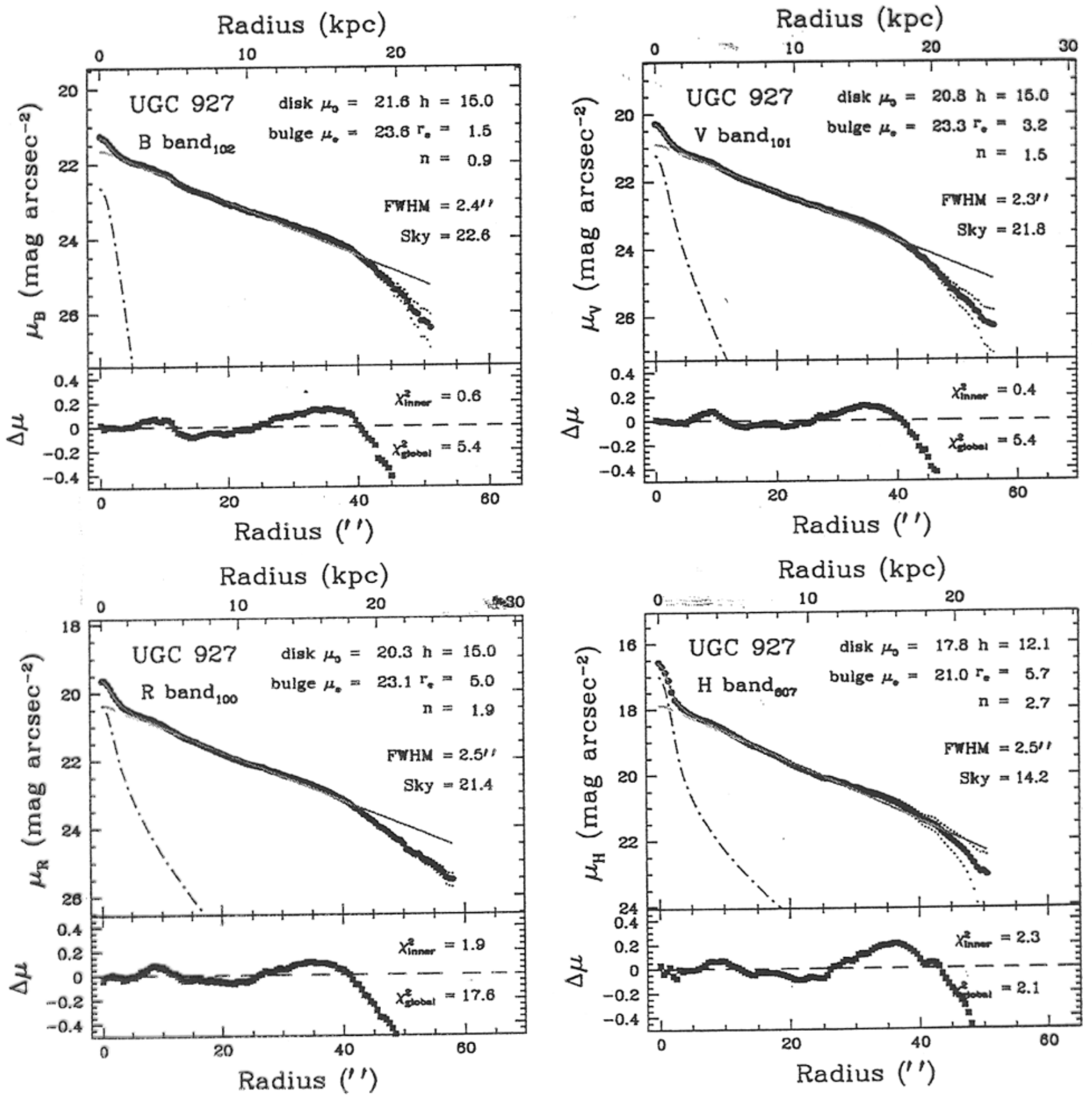

Fig. 13.— Decomposition results for a galaxy with a truncated disk (UGC 927). Note that sky errors could not account for the truncation.

M33: photometry

No bulge
Disk is "truncated": exponent up to 4.5 (8kpc) scale-lengths. Then it sharply declines

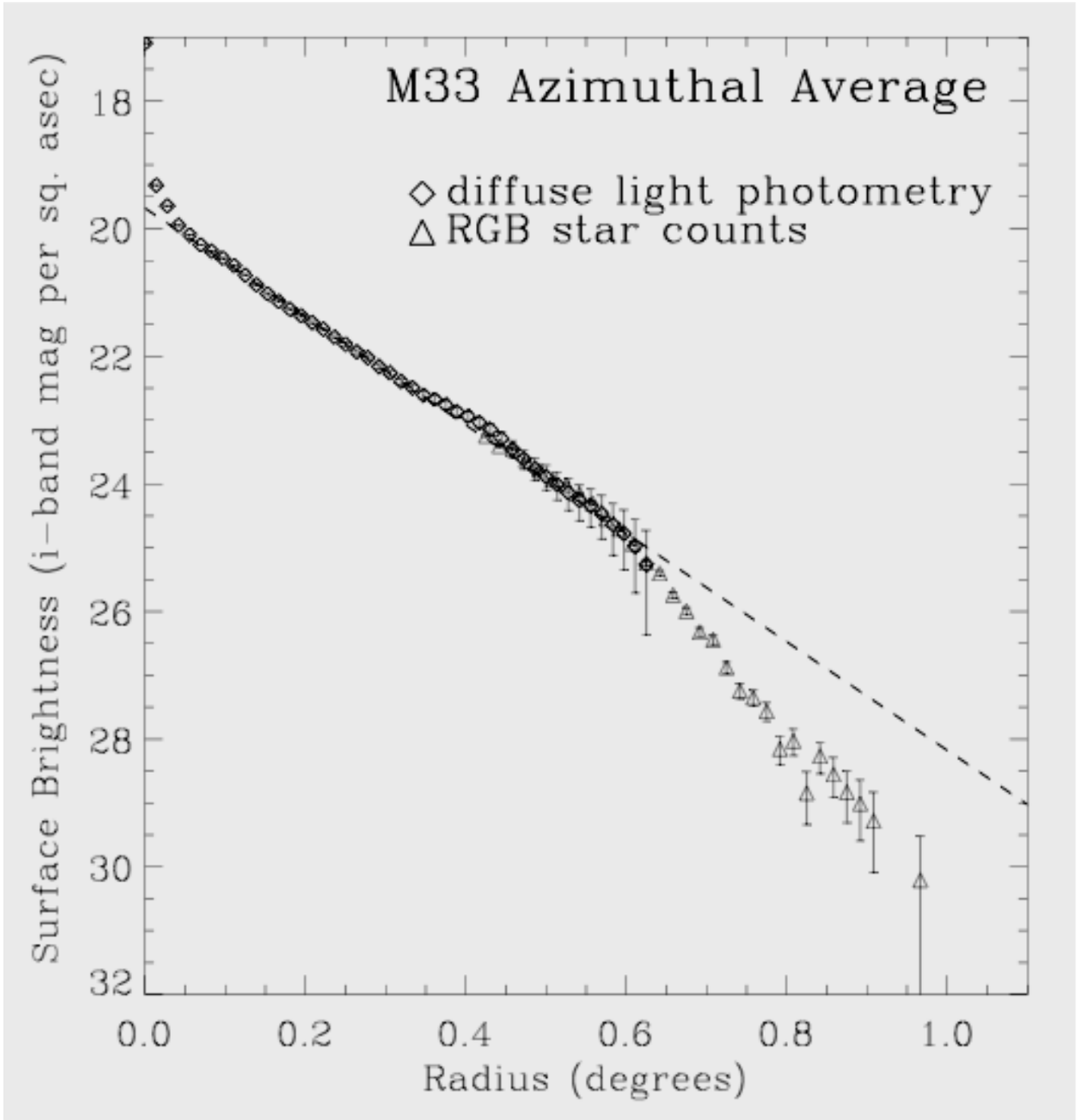

Ferguson et al. 2006

M_v =-18.9mag
$V_{rotation}$=100km/s

Global correlations: slope of Sersic profile for different morphological types and B/D.

Bulge gets steeper for earlier type and for spirals with larger bulges

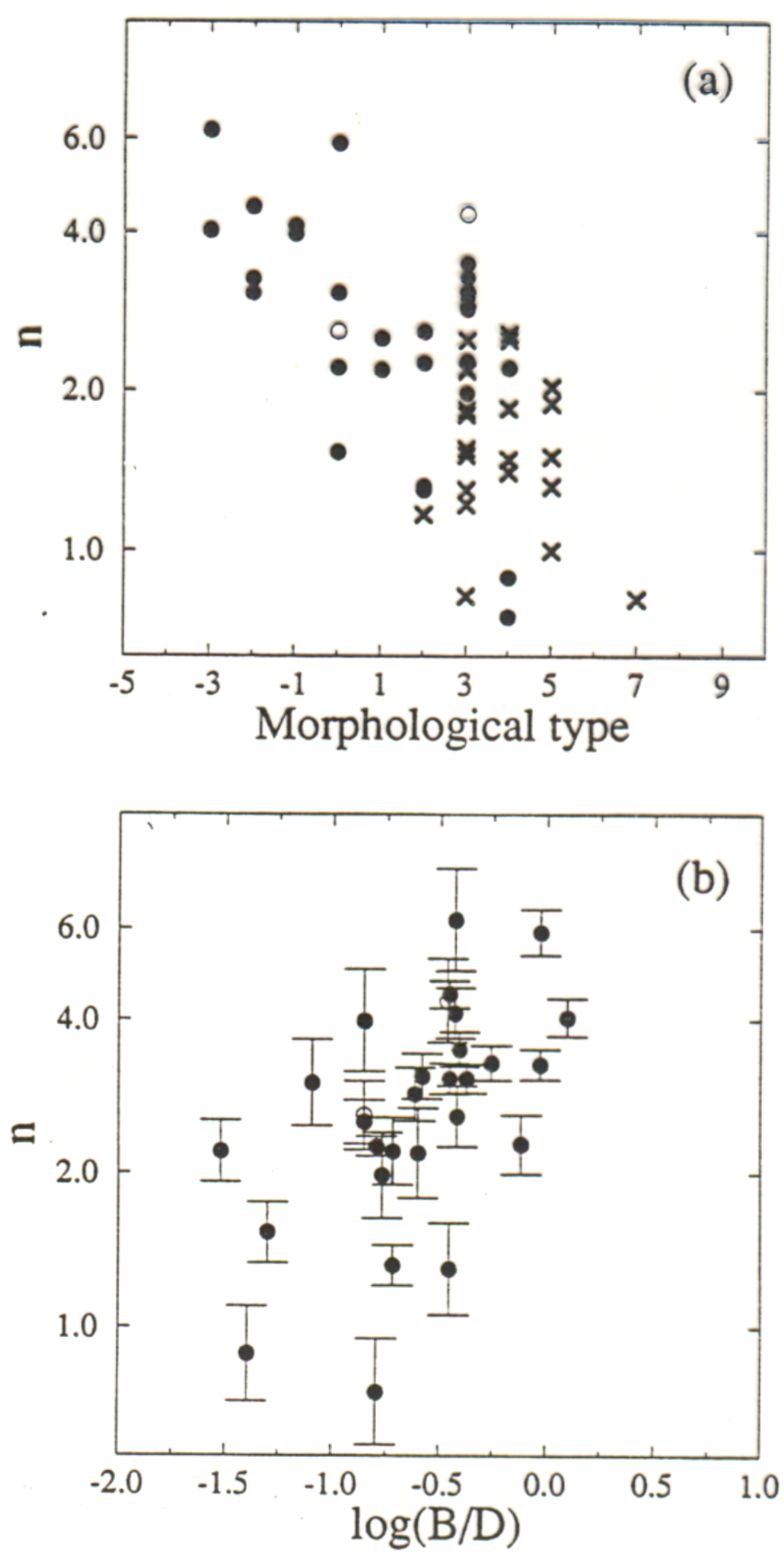

Figure 5. (a) The best-fitting n plotted (in logarithm) versus the morphological type of the galaxy. The galaxies of our sample are represented by the filled circles, the ones of Kent (1986) by crosses. The open circles indicate barred galaxies. No error bars are given in this plot, for clarity. (b) n versus bulge to disc ratio.

Distribution of disk scale lengths is relatively narrow

Courtesy

Examples:

MW: Rd =3kpc

M31: Rd =5.8kpc

For most of normal galaxies Rd is in the range of 3-6kpc

For dwarf irregulars Rd is (1-2)kpc

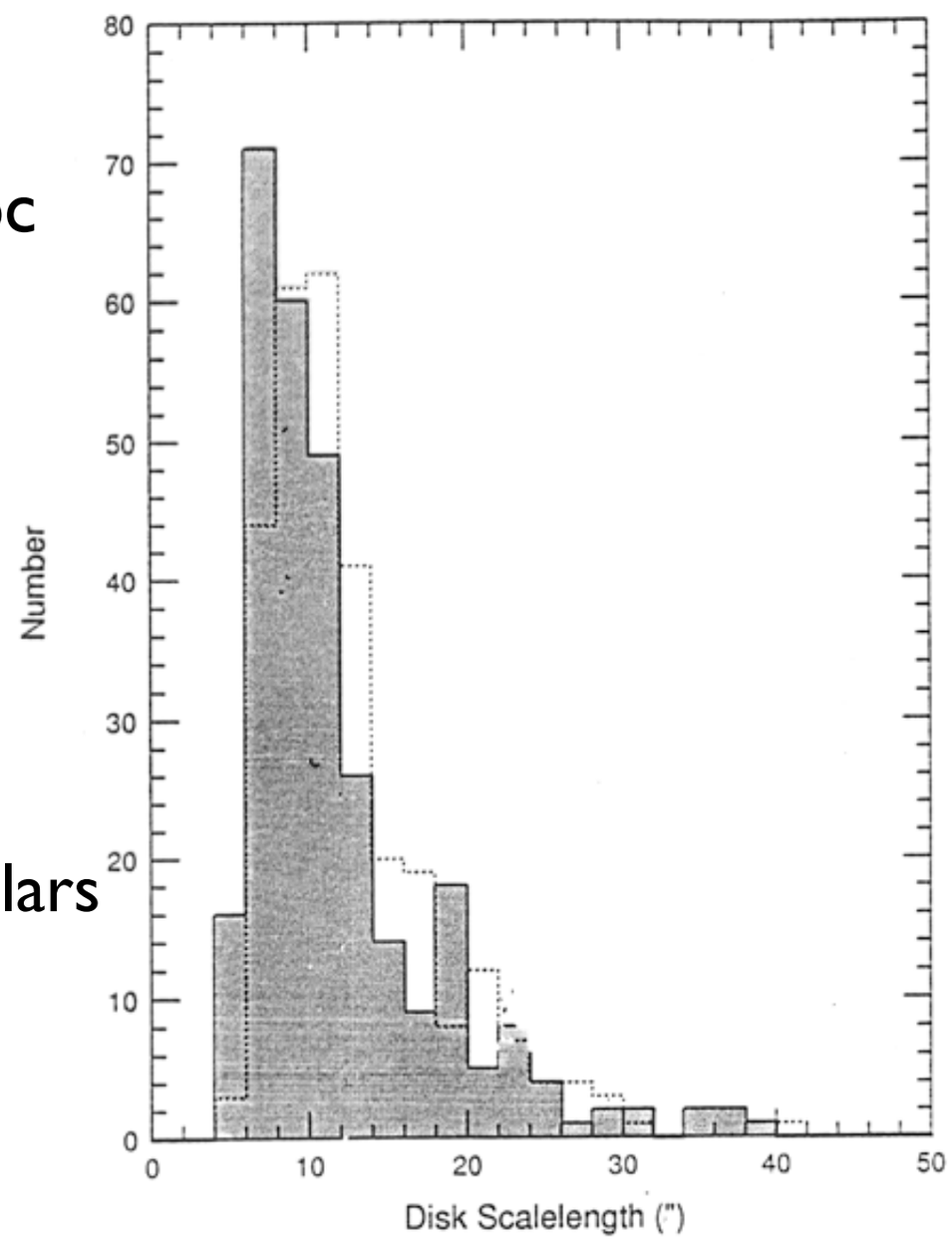

FIG. 11*a*

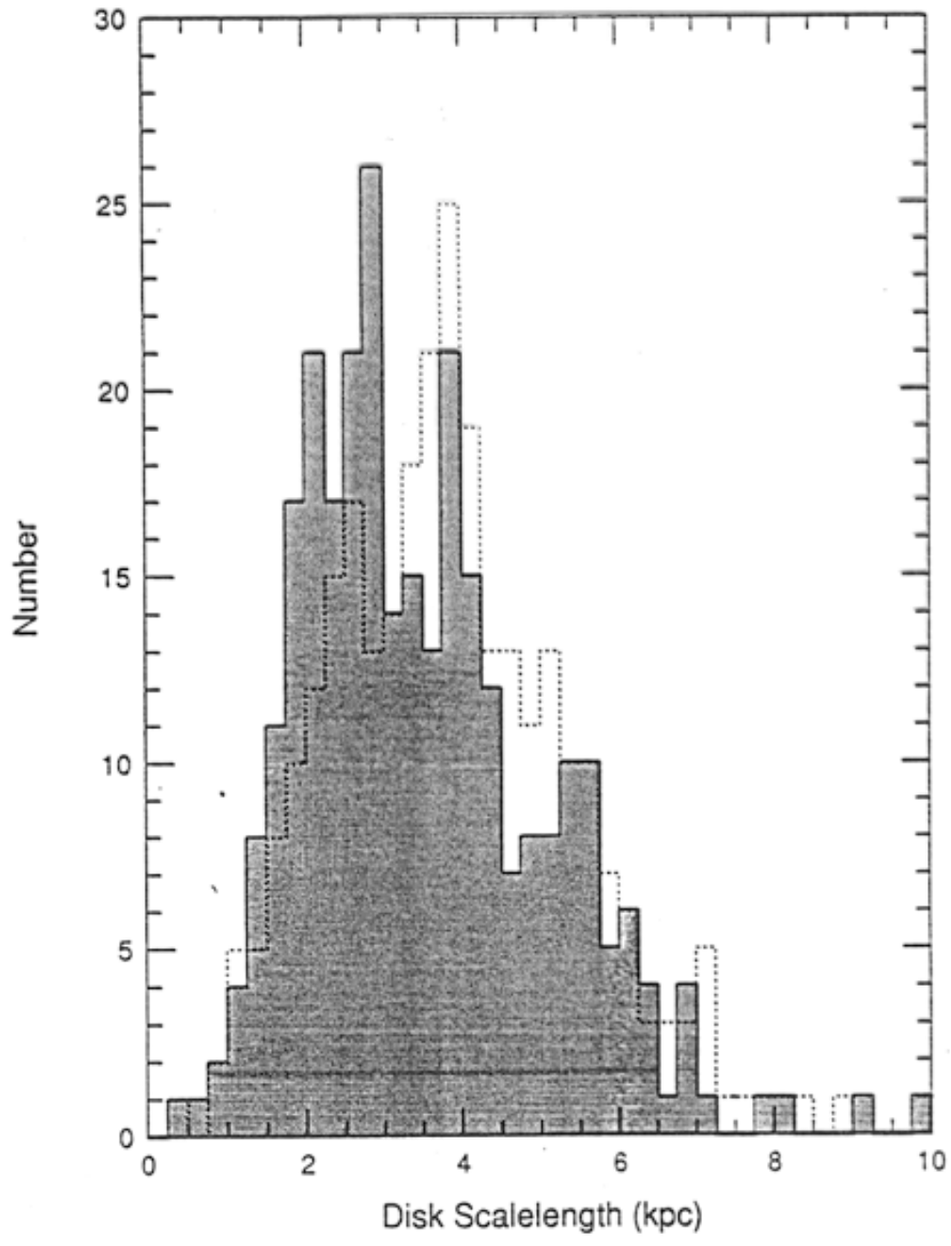

FIG. 11*b*

FIG. 11.—(*a*) Distribution of apparent disk scale lengths. Scale lengths measured by the "marking the fit" are represented under the shaded histogram. The dotted line denotes scale lengths measured through full B/D decomposition. See text for details. The pileup of galaxies at low *h* is due to the UGC diameter cutoff. It shows that 1′ galaxies typically have scale lengths of order 8″. (*b*) Distribution of absolute disk scale lengths. Same as Fig. 8, but scaled in distance using heliocentric redshifts and a Hubble constant of 80 km s^{-1} Mpc^{-1}. The catalog limit naturally disappears, and the distribution is more normally dispersed.

Courteau 97 AJ, 114, 2402

$V_{2.2} = V(2.2 R_{opt})$?
$= V_{max}$

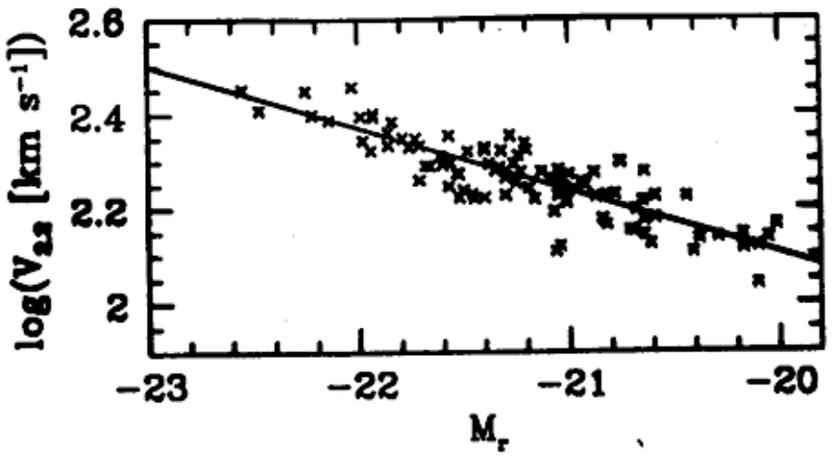

← TF
$M \simeq 7.5 \log V + C$.

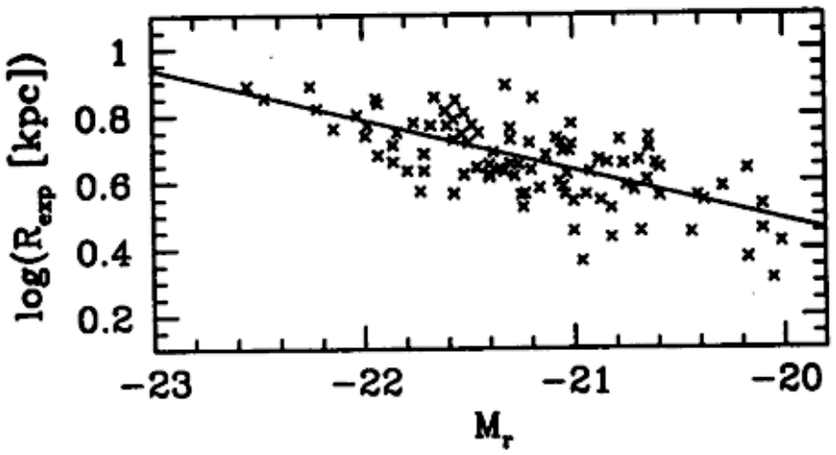

Size-Mag.

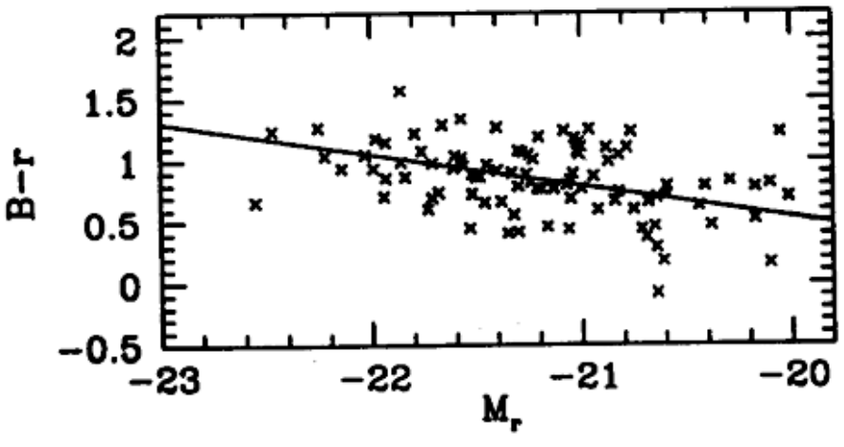

← Metallicity

Fig. 1.— Correlations of galaxy's rotational velocity, size, and color with absolute magnitude for our sample. The solid line corresponds to a robust fit by minimisation of the absolute data−model deviations. The fits assume equal weights at all points.

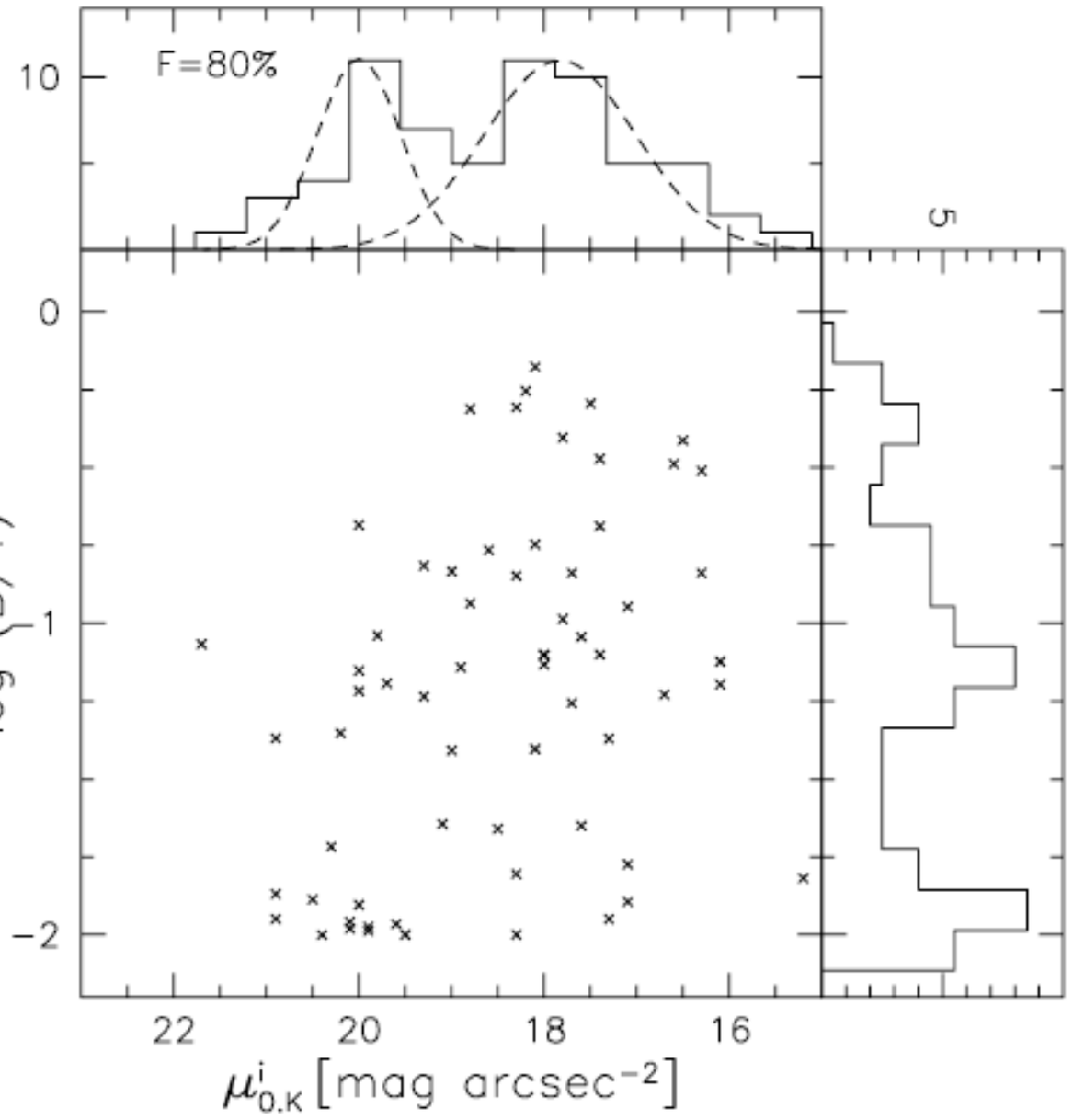

Figure 11. Distribution of inclination-corrected K'-band disc central surface brightnesses, $\mu^i_{0,K}$, as a function of bulge-to-total ratio, B/T, for the sample of 65 UMa galaxies.

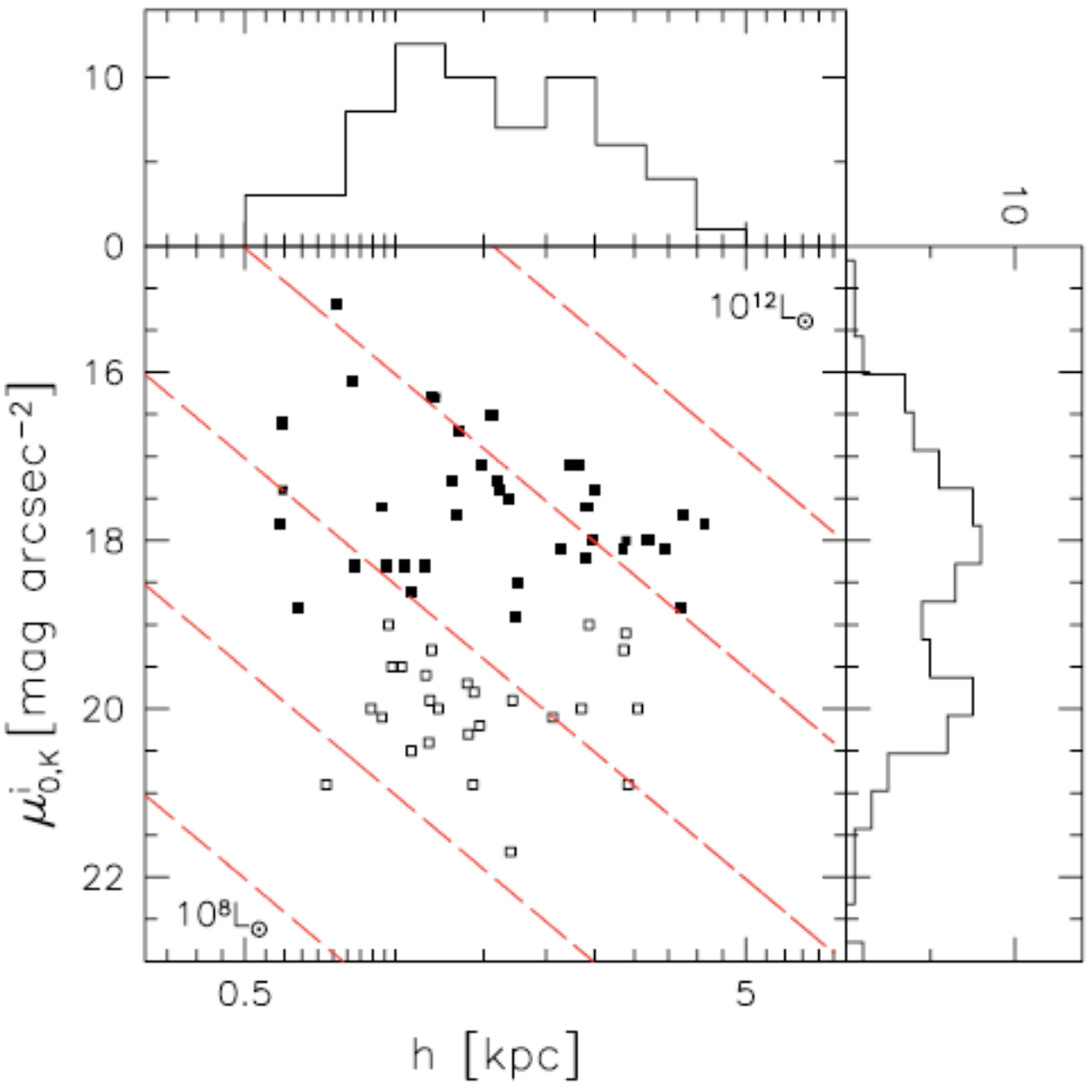

Figure 9. Distribution of inclination-corrected K'-band disc central surface brightnesses, $\mu^i_{0,K}$, as a function of disc scalelength, h, measured in kpc (using a distance to UMa of 15.5 Mpc) for the sample of 65 UMa galaxies. The long-dashed lines represent lines of constant total disc luminosity, while the different surface brightness classes are identified by open squares (LSB) and filled squares (HSB).

B/T ratios and Surface Brightness-disk scale length relations for Spirals.
Is there a bimodality?

McDonald et al 2009

Mon. Not. R. Astron. Soc. **393,** 628–640 (2009)

Case study: M31

Distance: 700 kpc
Disk scale length: 5.7 kpc in R band
Rotational velocity: 260 km/s

Disk mass: $7\times 10^{10}\ M_\odot$
Bulge mass: $2\times 10^{10}\ M_\odot$

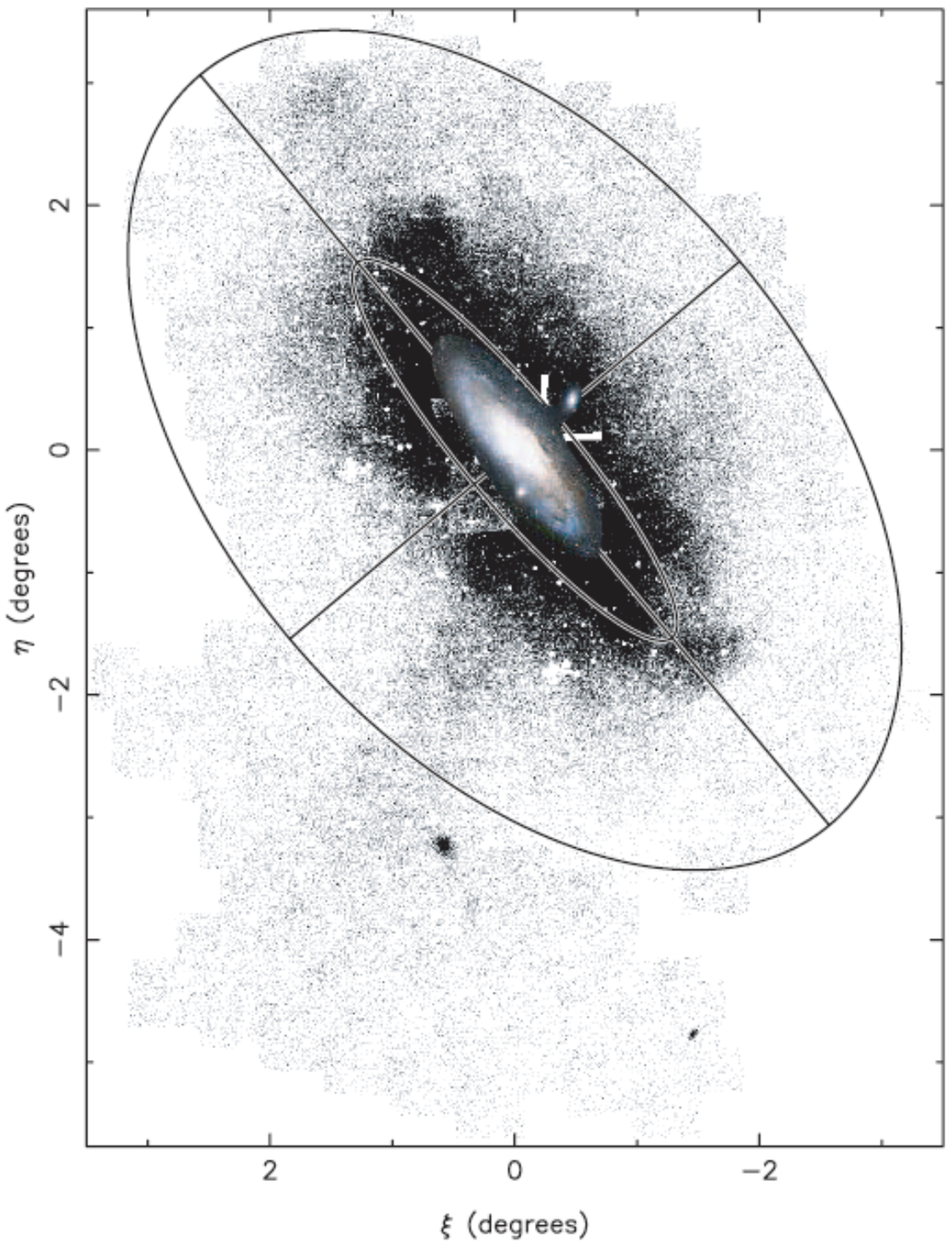

FIG. 1.—Current coverage of our large panoramic survey of M31 with the INT camera, in standard coordinates (ξ, η). The outer ellipse shows a segment of a 55 kpc radius ellipse flattened to $c/a = 0.6$, and the major and minor axis are indicated with straight lines out to this ellipse. A Digitized Sky Survey image of the central galaxy has been inserted to scale. The map shows the distribution of RGB stars throughout the halo. The most striking structure in the map is a vast flattened inner structure, of major axis extent ~4°, a messy inhomogenous entity that envelops the familiar bulge and disk of M31.

M3: bulge is a bar

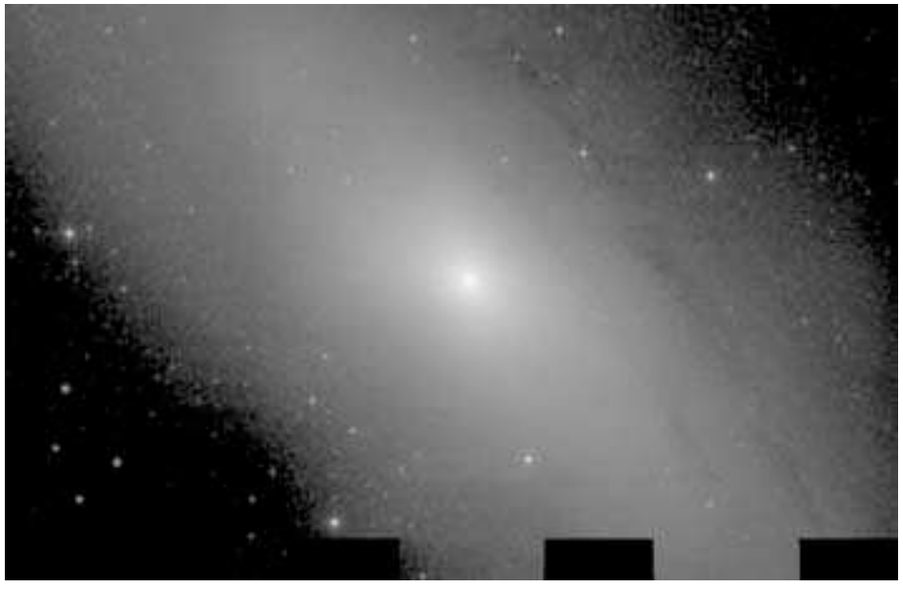

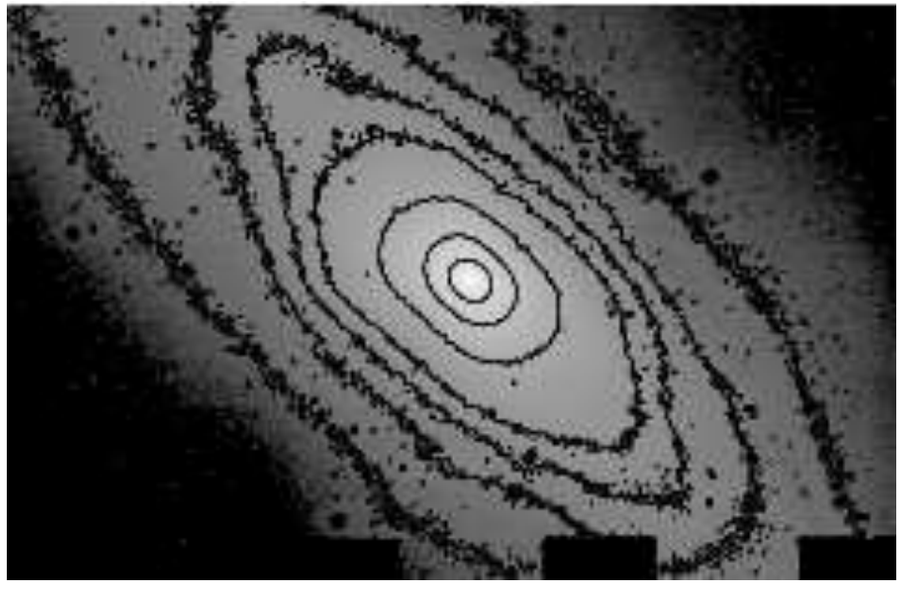

J-band image of the bulge region of M31 Athanassoula 2006

Case study: M31

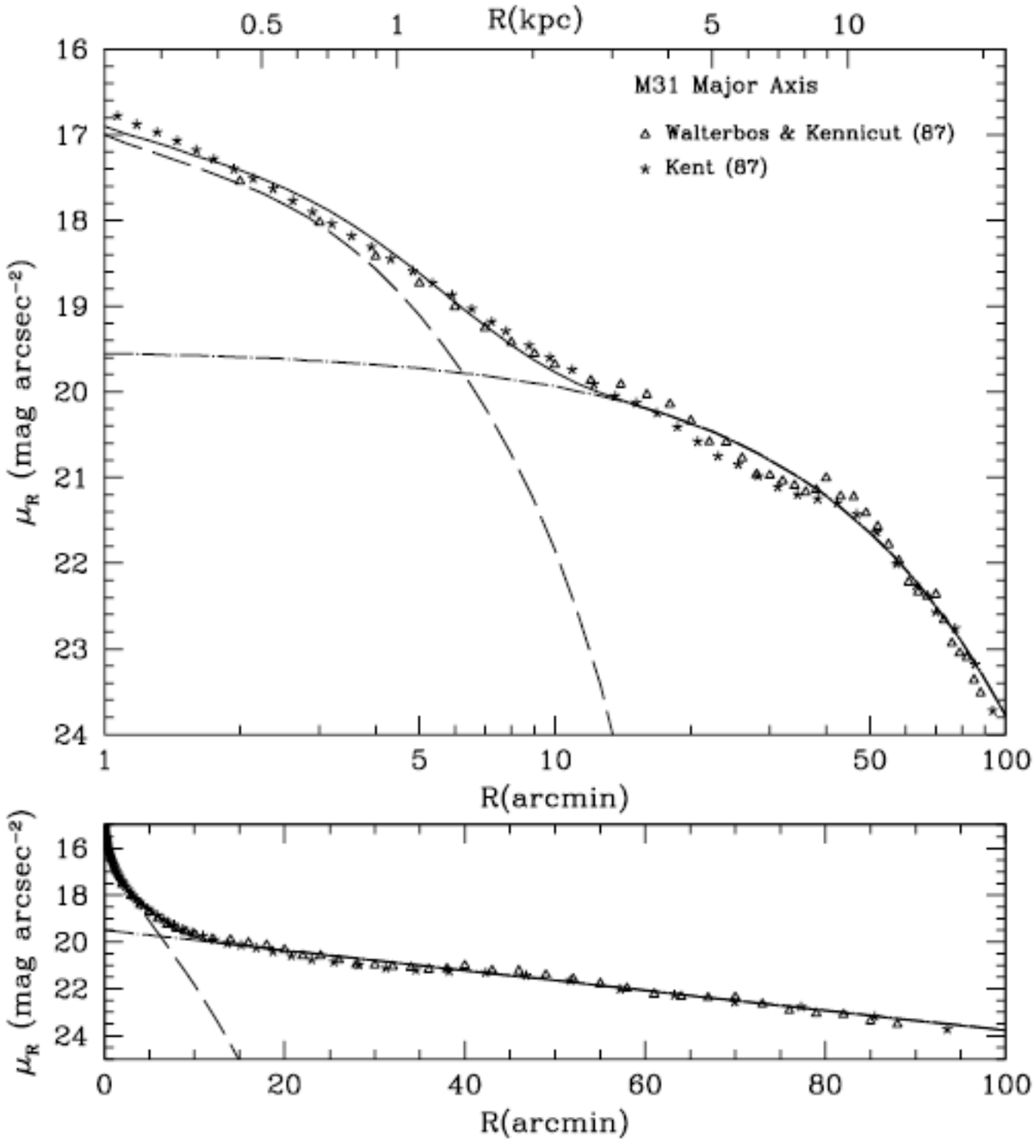

FIG. 5.—Surface brightness of M31 in the *R* band on linear (*bottom*) and logarithmic (*top*) scales. Deviations from the observational results are less than 0.2 mag.

M31

Stellar halo extends to 200 kpc. Some indications that outer halo was accreted: destroyed satellites

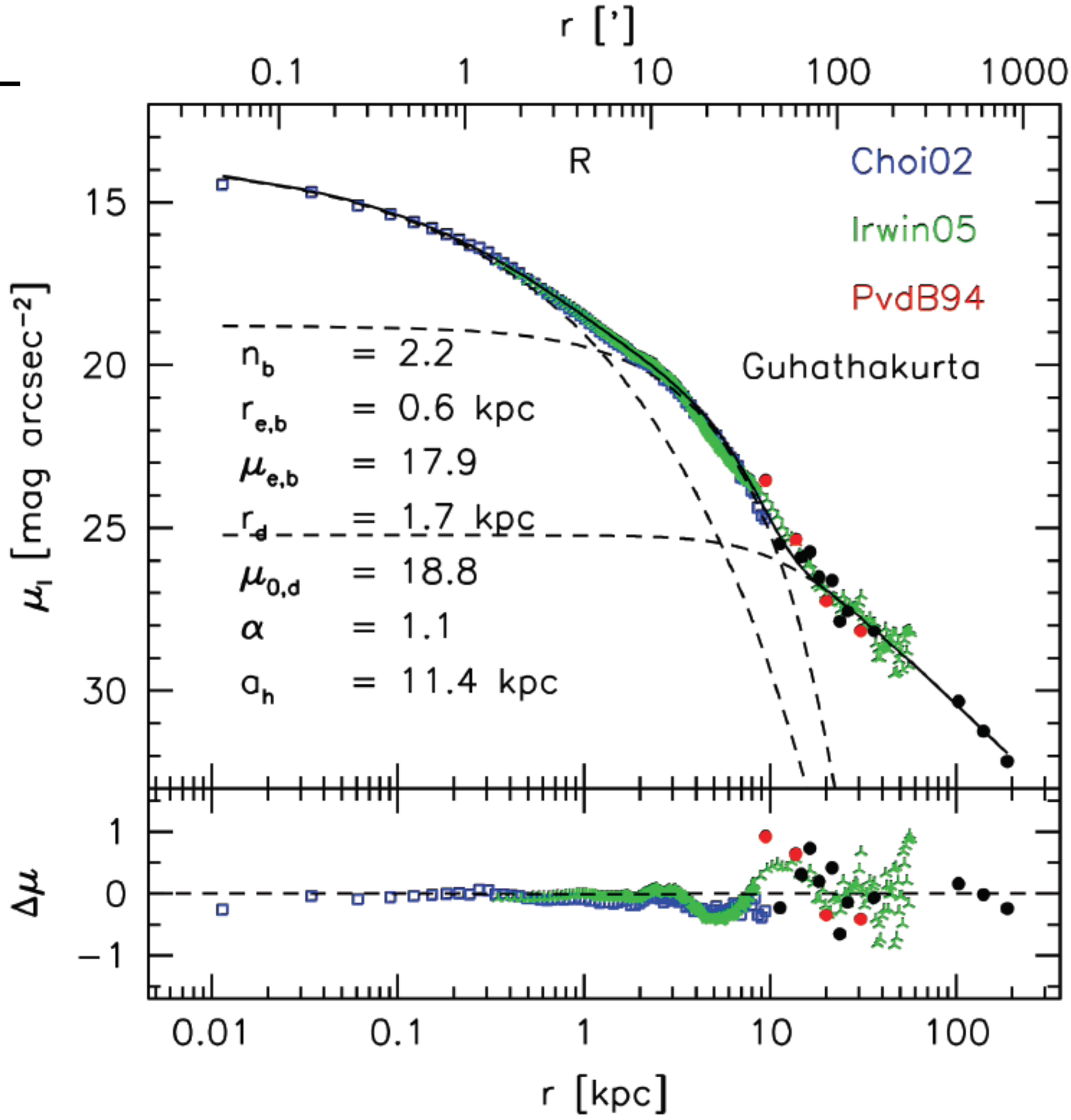

The remnants of galaxy formation from a panoramic survey of the region around M31

McConnachie et al 2009, Nature 461, 66

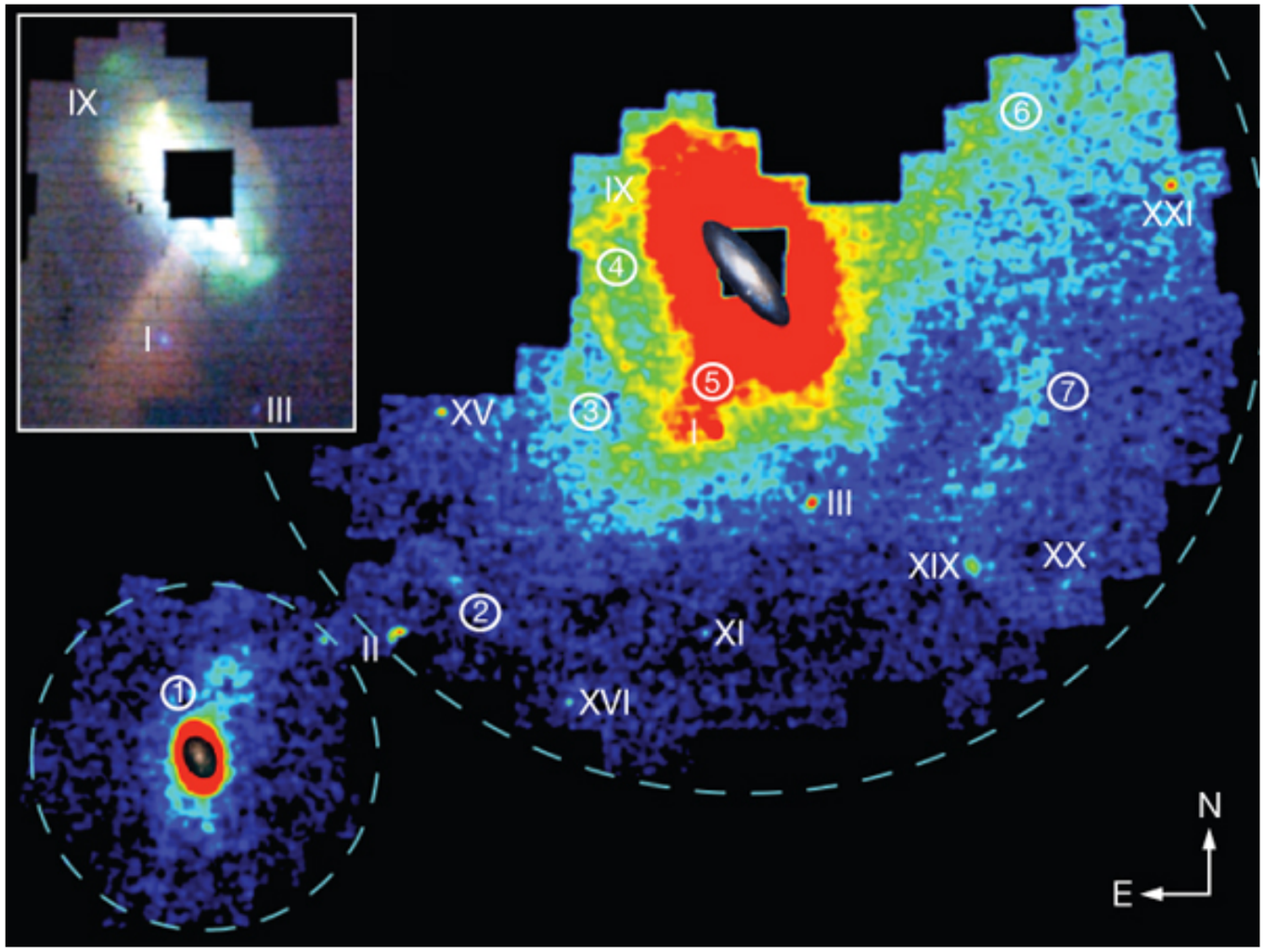

A tangent-plane projection of the density distribution of stellar sources in our extant PAndAS imaging is shown, with colours and magnitudes consistent with RGB stars at the distance of M31. The inset shows the central parts of our survey at higher resolution. Dashed circles represent the maximum projected radii of 150 and 50 kpc from M31 and M33, respectively. Scale images of the disks of M31 and M33 are overlaid. Visible dwarf satellites are indicated with roman numerals. Numbers in circles indicate the largest and most obvious substructures detected in a visual inspection of the image: 1, M33 structure; 2, 125-kpc stream (stream A); 3, stream C; 4, eastern arc (stream D); 5, giant stellar stream; 6, northwest minor-axis stream; 7, southwest cloud. Features 1, 6 and 7 (and part of 4) are new discoveries. Stellar sources were identified by using star–galaxy classification techniques described previously. Candidate RGB stars were selected by their position in a colour–magnitude diagram relative to theoretical isochrones for a 12-Gyr population at the distance of M31, using only stellar sources with $i_0 < 23.5$. A projection of the stellar density distribution within a putative metallicity range $-2.5 < [Fe/H] < -0.6$ dex was created with $0.02° \times 0.02°$ pixels, smoothed with a Gaussian filter with dispersion 3 arcmin, and displayed with square-root scaling. The inset was created by combining, with a red–green–blue colour scheme, three such maps of M31 with metallicities of $-0.4 < [Fe/H] < +0.2$ dex, $-1.3 < [Fe/H] < -0.4$ dex and $-2.3 < [Fe/H] < -1.3$ dex, respectively (each with $0.01° \times 0.01°$ pixels, smoothed with a Gaussian filter with 2 arcmin dispersion) and displayed with logarithmic scaling. Not all structures are visible with this (or any other) choice of metallicity cut, filter and scaling.

The remnants of galaxy formation from a panoramic survey of the region around M31

McConnachie et al 2009, Nature 461, 66

The evolution of M33 about M31 along an orbit consistent with the angular positions, distances[26] and radial velocities of M31 and M33 and with M33's proper motion[23]. Here, M33 starts 3.4 Gyr ago at a distance of $r \approx 200$ kpc on the far side of M31 falling down the line of sight (Z) to the Milky Way. After 800 Myr, M33 reaches pericentre and proceeds across our line of sight towards the southeast, reaching apocentre about 900 Myr ago before falling back towards M31 to its current position. Dots tracing the orbit are separated by 49 Myr to give a sense of the speed along the orbit. The lower inset shows a perpendicular view of M33's orbit. **b**, Quantification of the expected K-band surface brightness of M33 at different times from face-on and edge-on perspectives. The inner red/orange region with $\mu_K < 22$ mag arcsec^{-2} defines the size of the usual optical disk of M33 seen in images. The initial equilibrium models[30] for the two galaxies consist of a disk, bulge and dark-matter halo with structural parameters that accurately reproduce the observed surface brightness profiles and rotation curves. Because the mass profile of M31 beyond 100 kpc is not well constrained by observations, we appeal to cosmological arguments[24] that predict a mass of 2.5×10^{12} solar masses within $r < 280$ kpc.

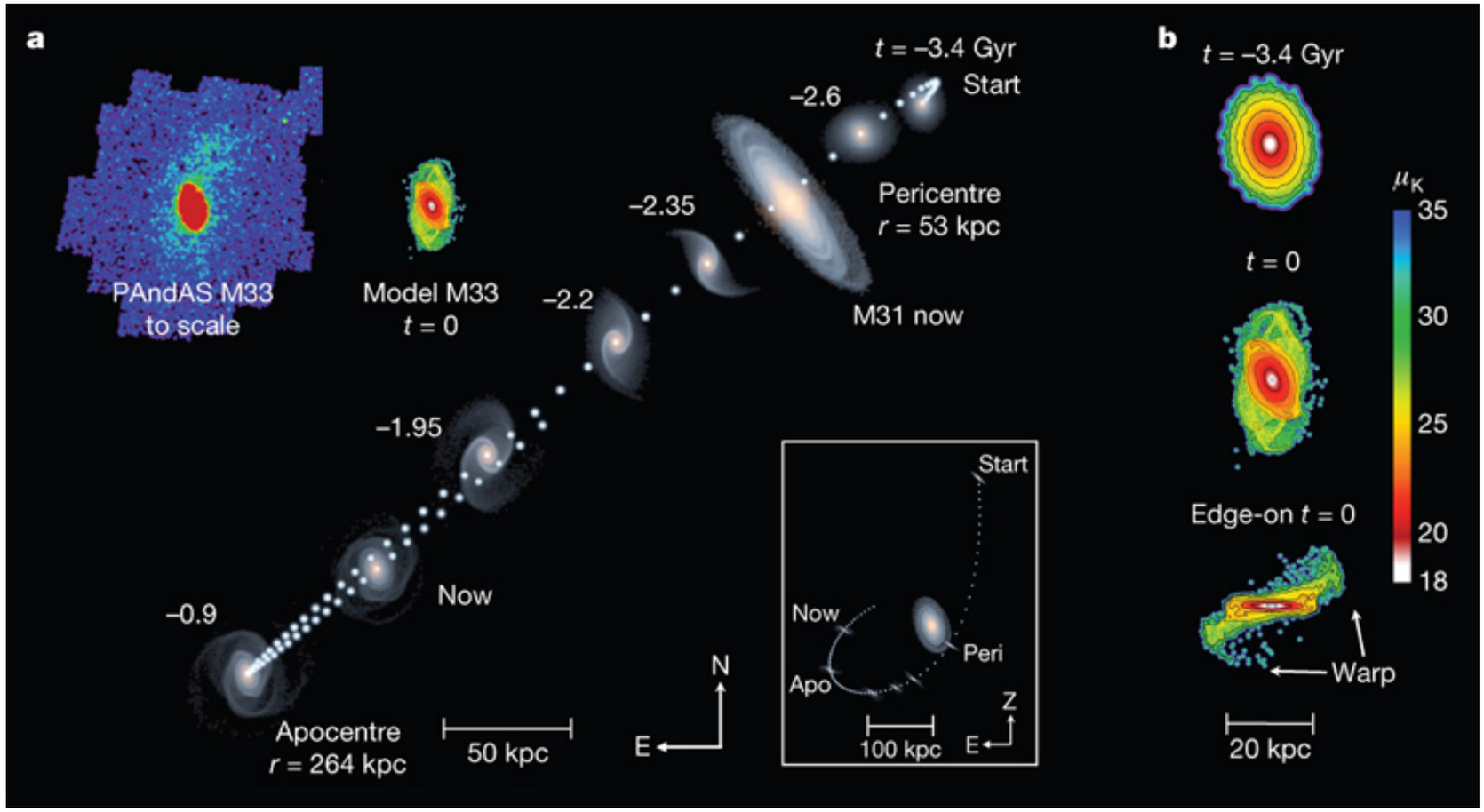

NGC 891: streams and tidal tails

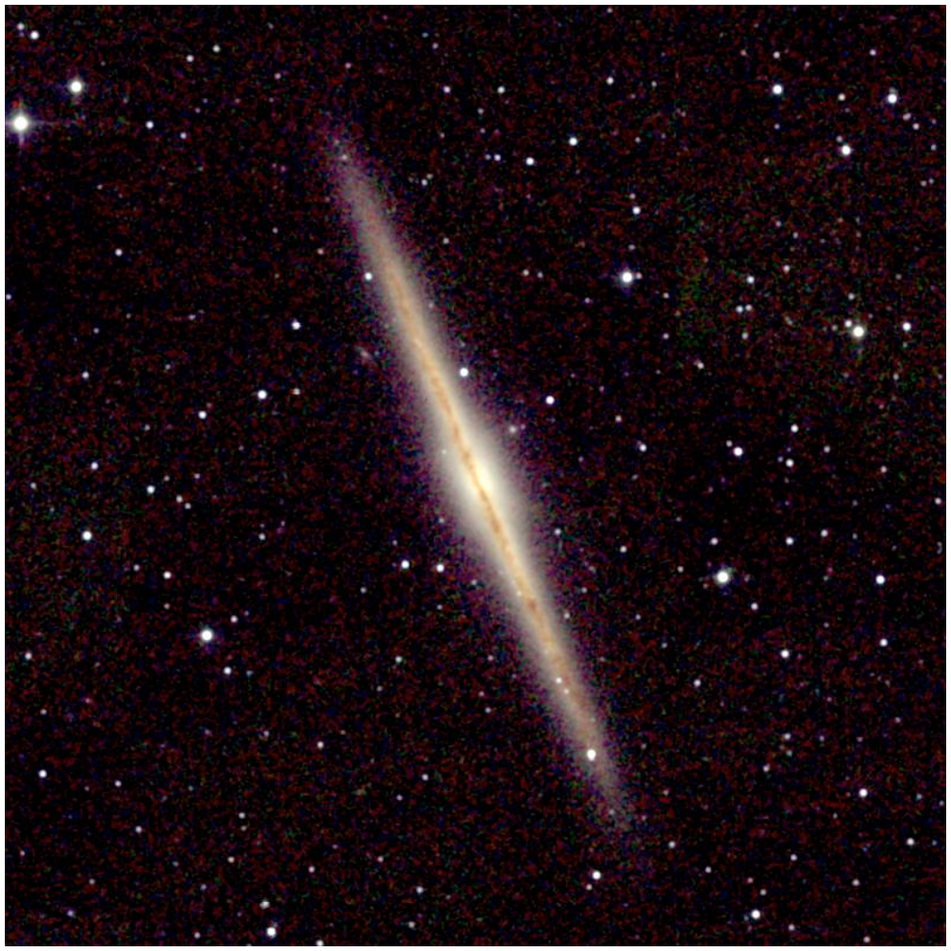

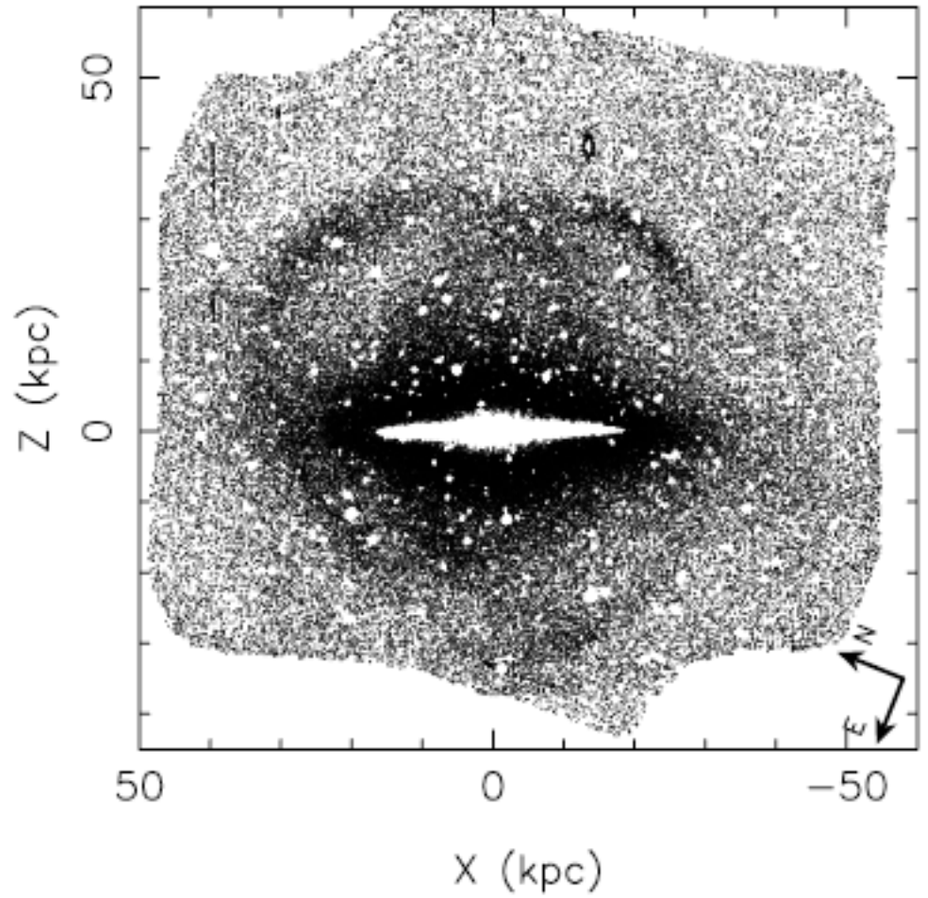

Figure 1. Surface density map of RGB stars over the surveyed area around NGC 891. The over-densities of old RGB stars detected in the present study reveal a large complex of arcing streams that loops around the galaxy, tracing the remnants of an ancient accretion. The second spectacular morphological feature is the dark cocoon-like structure enveloping the high surface brightness disk and bulge.

The bulge and the disk of the galaxy are found to be surrounded by a previously undetected large, flat, and thick cocoon-like stellar structure at vertical and radial distances of up to ~15 kpc and ~40 kpc, respectively.

Mouhcine et al 2010, ApJ 714, L12

Disk-bulge correlations

$r_{e,h}$ → radii of ½ luminosity

$\langle r_{e/h} \rangle = 0.22 \pm 0.09$

Exponential length: $h_{bulge}/h_{disk} = 0.13 \pm 0.06$

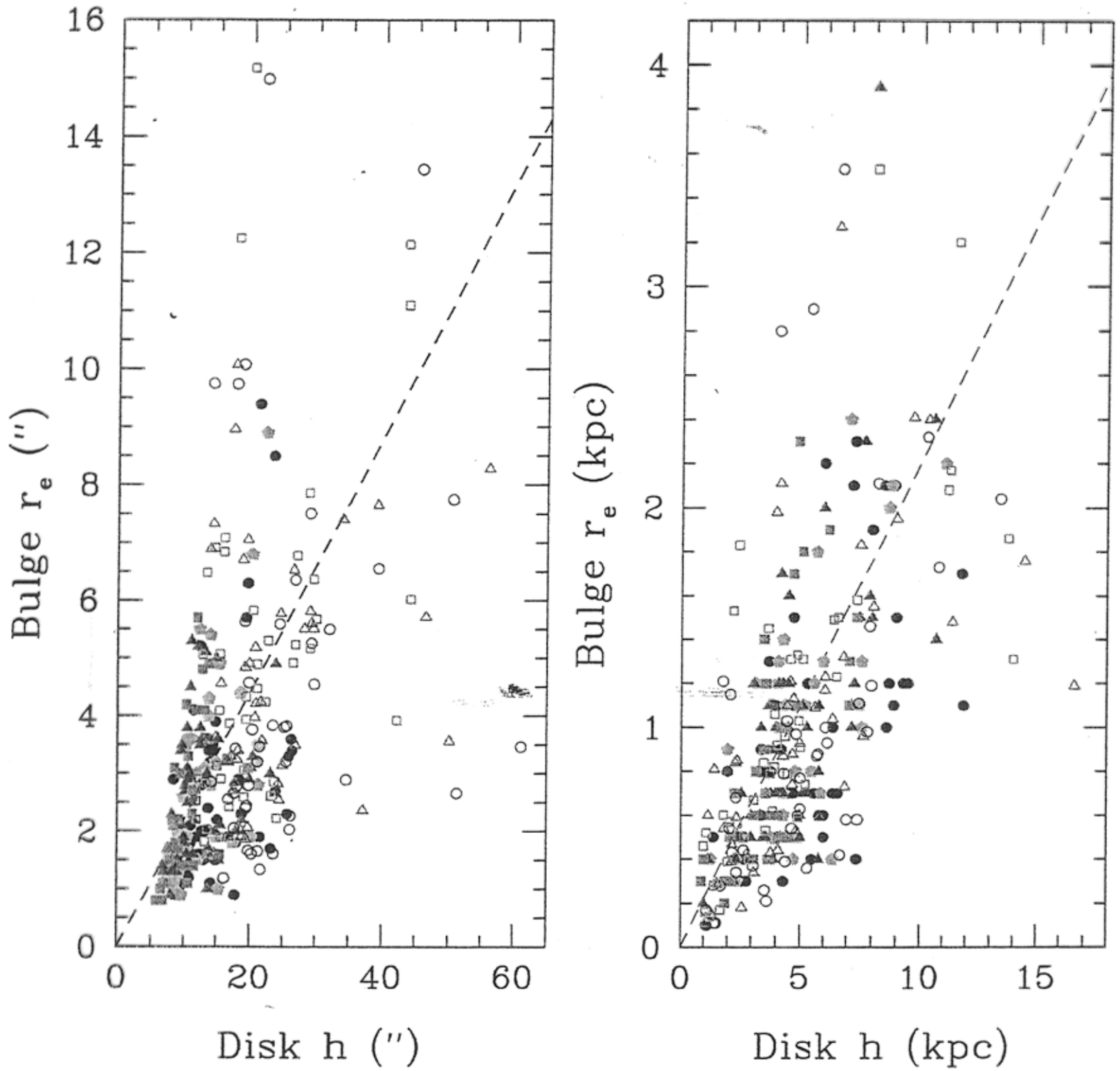

Color of bulges closely correlates with disk colors for Sb galaxies

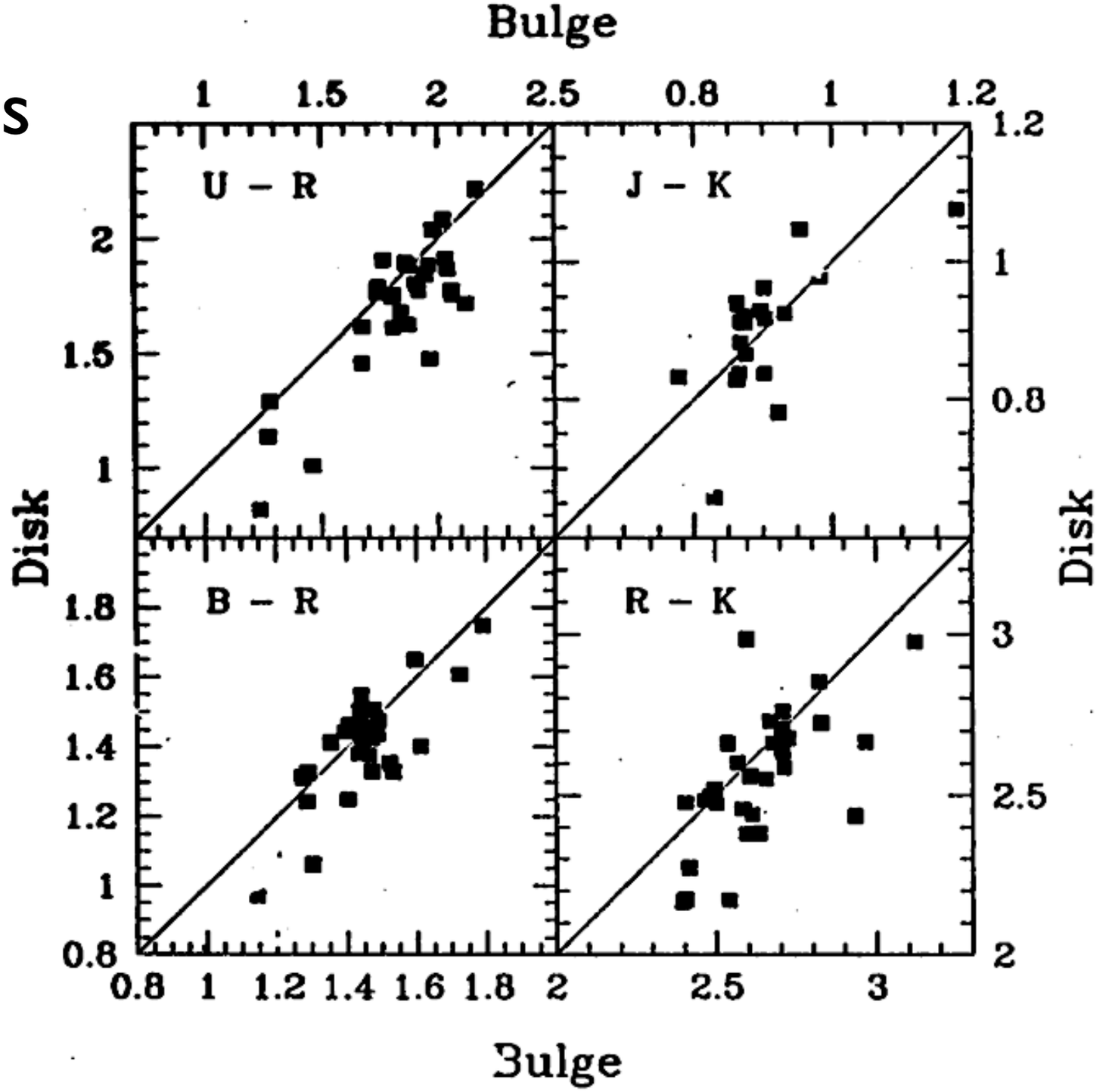

Figure 5. **Disk colors against bulge colors from Peletier & Balcells (1996). Bulge colors are measured at $r_e/2$ or 5″, whichever is larger, and disk colors are measured at 2 major-axis scale lengths. Color differences are, on average, of order $0^m.1$ for all passband combinations. Central colors are measured in special regions where extinction is minimal.**

Disk thickness: edge-on galaxies

Joachim, Dalcanton 2006, ApJ, 131,226

We model the surface brightness of each disk component as a radially exponential disk. We adopt the luminosity density L of each disk component to be

$$L(R,\ z) = L_0 e^{-R/h_R} f(z), \qquad (1)$$

where (R, z) are cylindrical coordinates, L_0 is the central luminosity density, h_R is the radial scale length, and $f(z)$ is a function describing the vertical distribution of stars.

Throughout, we adopt a generalized vertical distribution

$$f(z) = \mathrm{sech}^{2/N}(Nz/z_0), \qquad (2)$$

where z_0 is the vertical scale height and N is a parameter controlling the shape of the profile near the midplane. For appropriate choices of N, this equation can reproduce many popular choices for the vertical distribution of star light. With $N = 1$ equation (2) becomes the expected form for a self-gravitating isothermal sheet (Spitzer 1942; van der Kruit & Searle 1981a, 1981b, 1982). When $N \to \infty$, equation (2) reduces to $f(z) \propto e^{-z/h_z}$, where $h_z = z_0/2$. Previous fits to the vertical distribution

Disk thickness: edge-on galaxies

Joachim, Dalcanton 2006, ApJ, 131,226

Disk thickness correlates with the circular velocity:
larger galaxies have thicker disks.

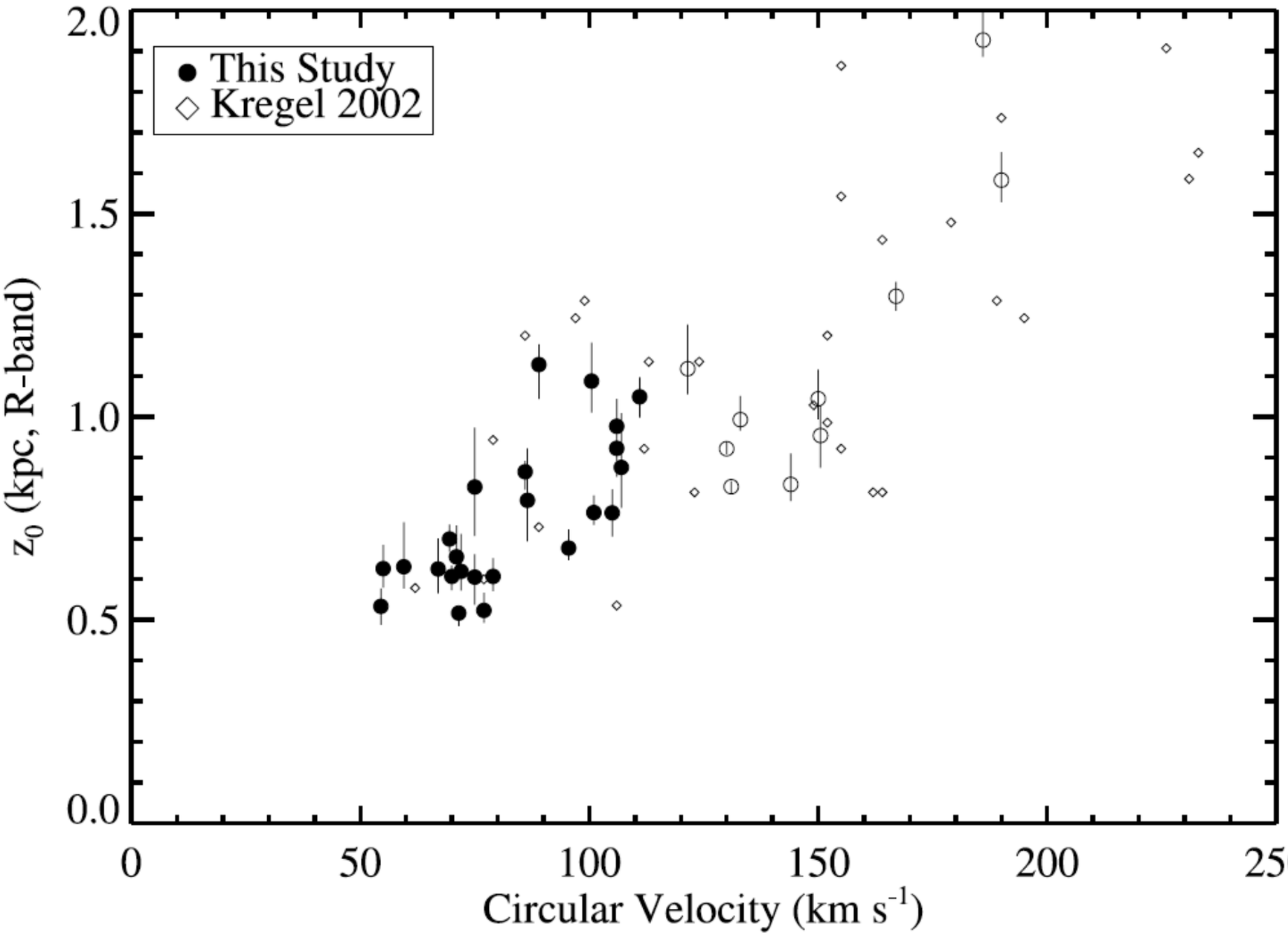

Galaxies typically have two components:

thin disk (hz =300-500pc)
thick disk (hz=1-2kpc)

Summary

- Two types of profiles: Freeman I (surface brightness increases monotonically) and Freeman II (surface brightness pause before it goes up in the bulge)
- ”1/4” law for bulges is a good fit for early type spirals with large bulges.
- Late type spirals are better fit with exponential bulges.
- On average the scale-lengths correlate: R_{bulge}/R_{disk} =0.13
- Disk scale lengths for normal galaxies are in the range 3-6kpc
- Dwarf irregulars have shorter scale-lengths: (1-2)kpc
- Bright galaxies are redder and more metal-rich.
- Colors of bulges and disks of late-type spirals correlate.